PCCP

Accepted Manuscript

ROYAL SOCIETY OF CHEMISTRY

www.rsc.org/pccp

Evidence for Intrinsic Nature of Band-Gap States Electrochemically Observed on Atomically Flat TiO_2(110) Surfaces

Shintaro Takata[1], Yoshihiro Miura[1] and Yuji Matsumoto[1,2*]

[1] Materials and Structures Laboratory, Tokyo Institute of Technology,
4259 Nagatsuta, Midori-ku Yokohama 226-8503, Japan

[2] Department of Applied Chemistry, School of Engineering, Tohoku University
6-6-07 Aramaki Aza Aoba, Aoba-ku Sendai,980-8579 Japan

[*] Corresponding author, e-mail: matsumoto@atomol.che.tohoku.ac.jp

---

TOC

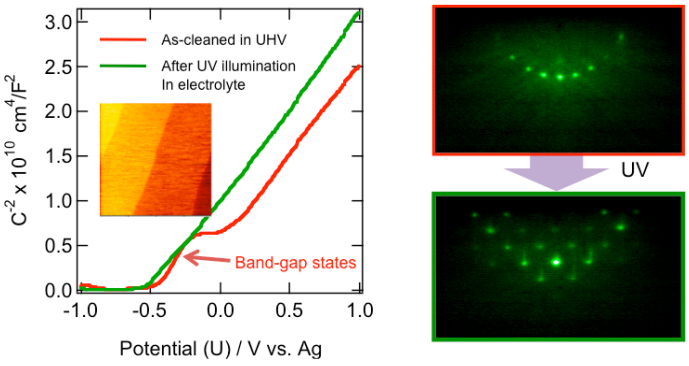

The intrinsic nature of band-gap states of UHV-clean TiO_2(110) single crystal and film surfaces were electrochemically investigated by UHV-electrochemistry approach.

Abstract

By an ultra-high vacuum (UHV) electrochemistry approach with pulsed laser deposition (PLD), we investigated the band gap state for TiO_2 (110). In the PLD chamber, a TiO_2(110) surface was cleaned by annealing in O_2 enough to exhibit a sharp (1x1) reflection high energy electron diffraction (RHEED) pattern. The cleaned TiO_2(110)-(1x1) sample then underwent electrochemical measuremnts without exposure to air, showing the band gap state at -0.14V vs. Ag by Mott-Schottky plot analysis. The band gap state was gradually disappeared under UV illumination at +0.6V vs. Ag due to photoetching and reappeared by reducing in a vacuum and/or depositing a fresh TiO_2 film. These results indicated that the electrochemically observed band gap state for TiO_2(110) was defect states due to oxygen deficiency, most probably identical to that observed in UHV, which dose not necessarily exist on the surface. The quantitative analysis of the defect density suggests that the origin of this defect state be not the surface bridging hydroxyls or oxygen vacancies, but rather the interstitial Ti^{3+} in the subsurface region.

Introduction

Titanium dioxide (TiO_2) has been one of the most attracting metal oxides because of its various functionalities widely applicable, including, for example, catalysis[1], photochemistry[2,3], dye-sensitized solar cells[4], gas sensing, and transparent conducting electrodes[5] that are sometimes greatly influenced by the inherent nature of its oxygen nonstoichiometry. In its fully oxidized form, TiO_2 is insulating with a wide band gap of around 3eV, the exact value of which depends on its kinds of polymorphs such as anatase, rutile and brookite. Once TiO_2 is situated in a reducing condition, there can be many oxygen vacancies and the related defects produced on the surface as well as in the bulk. One of the key issues related to the oxygen nonstoichiometry is the band gap state, understanding the origin of which is important not only from a basic science point of view, but also for a reproducible performance of specific TiO_2 applications.

There has been a long controversy about the origin of the band gap state experimentally and theoretically investigated so far. Conventionally the oxygen vacancy derived state in the band gap as is

found at ~0.85eV below the Fermi level (E_F) by photoelectron spectroscopy in redued-TiO_2(110) has been attributed to bridging oxygen (Obr) vacancies[6,7]. This O-vacancy model relies largely on experimental facts that the defect state will disappear by O_2 exposure[7]. An alternative origin of these defects was also proposed: the subsurface interstitial Ti^{3+} (Ti_{int}) is responsible for the defect state in the band gap[8,9]. The main basis for this assertion is the observation of different re-oxidation behavior of two defect states observable below E_F in the photoelectron spectroscopy, combined with scanning tunneling microscopy experiments: when re-oxidized the well-known peak at ~0.85eV, as is believed to be from the Obr vacancies, disappears much more slowly than that at ~10.8eV originated from the OH3σ which is produced when water molecules fill and replace the Obr vacancies. However, it is still controversial between these two different defect models for the band gap state[10,11].

On the other hand, similar band gap states in TiO_2 single crystals have been also observed at the aqueous electrolyte interface in electrochemistry [12-14]. However, the origins of the surface states have been unclear. One reason for this is that most sample preparations were performed in air, but not in UHV, even though the electrochemical measurements in an inert gas such as a pure Ar. In this case, the effects of contaminants could not be completely ruled out in the discussion about the origin of the surface states. In fact, for example, it is known that extrinsic surface states will be newly formed after the deposition of Fe atoms on the TiO_2 surface[15]. In addition, the electrochemically-observed surface states can be eliminated by UV illumination[14,16]. At that moment, it was inferred that, despite no direct experimental evidence, this was due to photoetching: the dissolution of TiO_2 resulted in the removal of the adsorbates forming the surface state at the same time. Therefore it has been considered that the electrochemically-observed band gap states may not be identical to those observed by photoelectron spectroscopy in UHV, and there has been little positive arguments about the origin of the band gap state by comparison with one another so far.

Nevertheless, the advantage is that the electrochemical measurement employed for detecting such surface states is so sensitive that the surface states will be detected even for fully oxidized TiO_2 samples, as compared with the conventional surface analysis techniques such as photoelectron spectroscopy.

Only the problem is the effects of the contaminants due to the sample preparation in air. In order to overcome this situation, we take an ultra-high vacuum electrochemistry approach[17-20], constructing the pulsed laser deposition-electrochemical cell (PLD-EC) system sketched in Fig. 1. More details can be found in ref. (21, 22), but this system enables us to investigate the origin of the band gap state by electrochemical measurements for clean TiO_2(110) samples prepared in UHV. The main features are as follows: (i) The TiO_2(110) single crystal can be annealed in O_2 as well as UHV; (ii) reflection high energy electron diffraction (RHEED) is used to characterize the sample surface; (iii) the layer-by-layer growth of epitaxial TiO_2 films is possible by PLD with in situ monitoring of RHEED intensity oscillations; (iv) the samples can undergo electrochemical measurements without exposure to air in a repeated manner by transferring the sample back-and-forth between the PLD and EC chambers. Further, as shown in the inset atomic force microscopy (AFM) image of Fig. 1, we use our originally developed 0.5wt% Nb-doped TiO_2(110) single crystals that exhibits an atomically flat steps-and-terraces structure, in which the surface factor can be assumed to be unity, and moreover that have no impurities except for carbon, as confirmed by x-ray photoelectron spectroscopy[23].

In this work, we tried to carefully investigate the band gap state electrochemically observed on such atomically flat TiO_2(110)-(1×1) surfaces and concluded that it was intrinsic, originated not from any contaminats on the surface, but rather from the interstitial Ti^{3+} ions in the subsurface region.

Resuts and discussion

The TiO_2(110)-(1×1) surface was prepared by annealing the atomically flat Nb-doped TiO_2(110) single crystal in $1x10^{-5}$ Torr O_2 at 673K for 1h, leading to a very sharp RHEED pattern of spots along a Laue circle with the Kikuchi lines superimposed (Fig. 1), which is evidence for its fully-oxidized clean surface. A set of Mott-Schottky plots of this TiO_2(110)-(1×1) surface was obtained for various modulation frequencies before and after UV illumination (Fig. 2A) based on the equivalent series *RC* circuit, where the applied electrode potential *U* (V) was measured relative to a Ag electrode as a reference at room temperature. According to semiconductor physics theory, for an ideal case where, for

example, the dopant concentration is constant throughout the semiconductor and the permittivity of the semiconductor is independent of the experienced electric field when applied the electrode potential[16, 24, 25] the Mott-Schottky plot will exhibit a straight line, *i.e*. the values of C^{-2} are exactly proportional to U. However, this is not the case, nonlinear Mott-Schottky plots were observed in an electrode potential range of -0.25 to +0.25 V vs. Ag for the as-prepared clean TiO_2(110)-(1×1). The nonlinear behavior is basically identical to those previously reported in electrochemistry and has been attributed to a deep surface state in the band gap[12-14], as illustrated in Fig. 2B. In general, the electron trap-detrap process of this kind of deep states cannot follow during the measurement at higher modulation frequencies so that the apparent differential capacitance (dQ/dV) value will decrease with an increase of the frequency. In fact the observed frequency dependence of the nonlinear part in the Mott-Schottky plot was consistent wih this model: the values of C^{-2} for the nonlinear part increases at higher frequencies, but not for the other linear parts.

After UV illumination at +0.6V vs Ag for 10min in electrolyte, such a nonlinear part in the Mott-Schottky plots completely disappeared, showing almost no frequency dependence as far as measured in the preset frequency range. This result also is in good agreement with the previous ones and due to the photoetching[14, 16]. In fact, before and after UV illumination, the *in situ* RHEED patterns and *ex-situ* AFM images showed that the surface morphology becomes rough (S1). In order to closely examine such a photoetching process, the cyclic voltammogram (CV) was also recorded for each step of UV illumination (Fig. 3A). As the illumination time increased, the values of current density for the CV pair peaks at electrode potentials of about -0.8V vs. Ag, which may be assigned to the redox reaction of Ti(III) (hydr)oxide / Ti(IV) (hydr)oxide[26], was found to gradually increase (Fig. 3B). The current increase is attributable to the increase of the effective area of the electrode surface due to the surface roughening during the photoetching; the surface factor was estimated to be, at most, about 3 from the degree of the current increase. From these results, the present observed deep state is confirmed to locally exist near the surface region as a “surface state”.

Next, whatever the origin of this surface state is, in order to quantitatively discuss, we estimated the defect density of this surface state. As shown in Fig. 2A the frequency dependence indicates that the trap-detrap response of the deep surface state seems not to be able to follow at higher frequencies above 1000Hz. If this is the case, a simple analysis model, proposed by Tomkiewicz in 1979[12], could be applied to estimate the defect density by using the data at 1000Hz, though there may be more accurate analysis models including the frequency dependence behavior[14], and the detailed analysis is shown in S2. As a result, the surface state was found to locate at around -0.14V vs. Ag; when the surface factor was unity its defect density before UV illumination was calculated to be $(6.4\pm0.4)\times10^{14}$ cm^{-2}, using the value of the Helmholtz layer capacitance C_H 63μC/cm^2 [12]. The value of the obtained defect density is reasonably acceptable because the reported values in the previous works were $(6\pm2)\times10^{14}$ cm^{-2} [12] and 9.6×10^{13} cm^{-2} [14], respectively. After UV illumination it was then decreased to be, at least, $(4.8\pm0.8)\times10^{13}$ cm^{-2} even when the surface factor after the photoetching was assumed to be unity, and was different by almost one order of magnitude between before and after UV illumination. Fig. 4A also shows a systematically deceasing of the defect density for the surface factor of unity with UV illumination time for the photoetching process of Fig. 3. In both cases, it should be noteworthy that the values of the defect density before or just after a short UV illumination are quite large for the surface Ti atom density on TiO_2(110) (5.2×10^{14} cm^{-2}). If the surface state were originated from the adsorbates, no clear (1×1) RHEED pattern could be observed. In fact, as shown in Fig. 4A the defect density increased again after the reduction by annealing at 673K in UHV (Fig. 4B), and much more after the subsequent layer-by-layer growth of TiO_2 in a reducing condition by PLD from a single crystal target of TiO_2 (~10nm in 1×10^{-5} Torr O_2 at 673K) (Fig. 4C). Note that the defect density much increased after the growth of TiO_2 film, but the shallow donor density N_D near the surface region, which can be also estimated as well as the defect density of the surface state, markedly decreased (S3). In the Nb-doped TiO_2 single crystal, the donor density N_D corresponds to the doping level of Nb, ex. ~1.4×10^{20} cm^{-3} at a 0.5w% doping level, while it does to the density of bulk oxygen vacancies that make a shallow donor state in a thin film[27]. Thus, the amount of defect density is not so strongly related to that of such a

typical bulk oxygen vacancy. In a series of these treatments as shown in Fig. 4, there is little possibility to recontaminate the surface without air exposure, and therefore the surface state is intrinsically due the surface oxygen vacancy or its related defect states, similar to those observed by photoelectron spectroscopy in UHV.

In order to closely examine whether these two band gap states are identical or not, their energy levels were carefully compared. First, the energy levels of the band gap state have been so far determined from E_F in the photoelectron spectroscopy. However, E_F will change according to different reducing conditions, and therefore we should estimate the absolute energy level of the band gap state relative to either the conduction band minimum (CBM) or the valence band maximum (VBM). Wendt et al, who proposed the interstitial Ti^{3+} model, reported in photoelectron spectroscopy a substantial shift of the dominating features between binding energies of ~3 and ~9.5eV, which are primarily O2p-derived states, by ~0.4eV toward E_F when re-oxidized the r- and h-TiO_2(110) [8]. This suggests that the downward band bending should occur near the surface, i.e. E_F be above the CBM level by ~0.4eV for r- and h-TiO_2(110) and that the band then recovered almost flat with E_F matched to the CBM when re-oxidized. If so, the energy level of the band gap state in the photoelectron spectroscopy becomes ~0.45eV below the CBM since it is estimated to be ~0.85eV relative to E_F for such r- and h-TiO_2(110). On the other hand, the energy level of the band gap state electrochemically observed is ~ –0.14V vs. Ag, whereas the flat band potential U_{fb}, corresponding to E_F, is –0.54V vs. Ag, which was estimated from the Mott-Schottky plot after the photoetching. Assuming that E_F almost coincides with the CBM, as is often the case with highly conducting TiO_2, the energy level of the band gap state becomes thus ~0.40V from U_{fb}, i.e. below the CBM. In previous works, the energy levels of the band gap states were also electrochemically estimated: according to Kobayashi et al it was ~0.5V below the CBM for a TiO_2(110) single crystal [14], though in some of other experiments what kind of crystal planes of TiO_2 they used is not clearly stated and the energy levels are ranged from 0.8 to 1.2V below the CBM [12, 13]. From these results, among which have two defect states almost the same energy level in the band gap, it is

reasonable to conclude that the band gap state electrochemically observed has the same origin as that in photoelectron spectroscopy.

Once it is accepted that these two band gap states are identical, we may take some insight into the origin of this surface state. The simple, but quantitative analysis suggests that the defect density of ~6×10^{14} cm^{-2}, even though it should depend largely on the value of C_H, is almost in the same order of magnitude as that of Obr atoms on TiO_2(110) (5.2×10^{14} cm^{-2}). Taking it into account that one Obr vacancy produces two electrons as a donor, the Obr vacancy density can reach, in this case, as large as ~50% in coverage. This is not probably the case because the TiO_2(110)-(1×1) surface used in electrochemical measurements is prepared in oxidizing condition and immersed in water solution and almost no Obr vacancies should remain on the surface. On the other hand, the bridging hydroxyls are also known as the major contributor to band gap states[10 11]. However, the possibility of the surface hydroxyls to explain such a large defect density may be ruled out. Even if such hydroxylation occurred, it would occur according to the amount of oxygen deficiency on the surface, which could not reach ~6×10^{14} cm^{-2} since the RHEED pattern exhibits a sharp (1×1) pattern of the fully-oxidized clean surface before Mott-Schottky measurements. Thus, the surface state, at least, electrochemically found in the band gap, is much more likely to have the origin of Ti_{int} atoms in the subsurface region. If this is the case, since even after 10min. photoetching to remove most of defect states, the steps-and-terraces structure was still visible as shown in S1, the photoetched region is likely to be within a few nm in depth from the surface, and the volume density of Ti interstitials is thus estimated to be, at most, on the order of 10^{21} cm^{-3}, the value of which seems reasonable as a volume density of Ti_{int} atoms.

Conclusion

In conclusions, we have verified that the surface state in the band gap observed at the TiO_2(110)/electrolyte interface is intrinsic, and most probably identical to that found by photoelectron spectroscopy in UHV. Even for a fully oxidized TiO_2(110) surface in an aqueous solution, the defect density of the surface state is in the order of 10^{14} cm^{-2}, which could be difficult to explain only by the

oxygen vacancy model. Therefore, at the moment the origin of this surface state would not be Obr vacancies, but rather Ti_{int} atoms in the subsurface region. Moreover, the UHV-electrochemistry approach employed in this work has been also demonstrated to be one of the promising techniques for the defect analysis on oxide semiconductor surfaces, in which both of the high sensitivity in electrochemical measurements and the high quality of the sample prepared in UHV can be achieved. Understanding the origin of and finding the way to control of the defects on oxide semiconductor surface will become more and more important to realize new oxide-based chemical or electronic devices utilizing its interface properties [28-30], to which this approach will to a large extent contribute in near future.

Methods

Experiments were performed on our originally developed PLD-EC system, using a KrF excimer laser (λ=248nm, COMPex 100) with a fluence of ~1.5J/cm^2. A 10nm-thick TiO_2 film was deposited at 673K in 1×10^{-5} Torr O_2 at 1Hz, and after the deposition the sample was cooled down to RT in the O_2. The primary electron energy for RHEED observations was 25keV. All the electrochemical measurements were performed in pure Ar gas (6N, Tokyo Koatsu Yamazaki Co., Ltd.) at normal pressure, using a threeelectrode electrochemical cell with 4N Ag and Pt wires (Nilaco) as reference and counter electrodes. The electrolyte solution was 1 M $HClO_4$ (purity > 4N for chemical analysis Kanto Kagaku), and PURELAB Ultra (Analytic, ORGANO) was used for pure water. Mott-Schottky plots were measured at different modulation frequencies and an amplitude of 10 mV with an Ivium CompactStat electrochemical and impedance analyzer. 0.5wt% Nb-doped TiO_2 (110) single crystals that were pre-treated to exhibit a steps-and-terraces structure were purchased from Shinkosya Co. After the Mott-Schottky measurements, the sample was washed in pure water in the EC chamber and transferred back to the PLD chamber. By annealing once more above 400 ^oC in 1×10^{-5} Torr O_2 the sharp RHEED pattern almost identical to that before electrochemical measurements was observed, indicative of its atomically

flat and clean surface with no surface etching[21]. To make an ohmic contact, the backside of the crystal was coated with In-Ga alloy, on which a Cu-foil was attached. The UV illumination was carried out with a high-pressure Hg lamp (USH-150SC(Ushio)), whose light intensity measured using an integral light counter for 254nm (UIT-150-A (Ushio)) was 28mW/cm^2. AFM images were measured on Seiko Instruments SPA-400.

Acknowledgements

This work has been partially supported by Grant-in-Aid from the Ministry of Education, Culture, Sports, Science and Technology of Japan (No.20360294).

References

(1) Haruta, M.; Kobayashi, T.; Sano, H.; Yamada, N. Novel Gold Catalysts for the Oxidation of Carbon Monoxide at a Temperature far Below 0°C. *Chem. Lett.* **1987**, 16 (2), 405-408.

(2) Fujishima, A.; Honda, K. Electrochemical Photolysis of Water at a Semiconductor Electrode. *Nature* **1972**, 238, 37-38.

(3) Fujishima, A.; Xintong, Z.; Donald, A. TiO_2 photocatalysis and related surface phenomena. *Surf. Sci. Rep.* **2008**, 63, 515-582.

(4) Grätzel, M. Photoelectrochemical cells. *Nature* **2001**, 414, 338-344.

(5) Furubayashi, Y.; Hitosugi, T.; Yamamoto, Y.; Inaba, K.; Kinoda, G.; Hirose, Y.; Shimada, T. and Hasegawa, T. A Transparent Metal: Nb-Doped Anatase TiO_2. *Appl. Phys. Lett.* **2005**, 86, 2521011-1-3.

(6) Henrich, V. E. and Cox, P. The Surface Science of Metal Oxides (Cambridge Univ. Press, Cambridge, 1996)

(7) Henrich, V. E.; Dresselhaus, G. and Zeiger, H. J. Observation of Two-Dimensional Phases Associated with Defect States on the Surface of TiO_2. *Phys. Rev. Lett.* **1976**, 36 (22), 1335-1339.

(8) Wendt, S.; Sprunger, P. T.; Lira, E.; Madsen, G. K. H.; Li, Z.; Hansen, J. ø.; Matthiesen, J.; Blekinge-Rasmussen, A.; Lægsgaard, E.; Hammer, B. and Besenbacher. F. The Role of Interstitial Sites in the Ti3d Defect State in the Band Gap of Titania. *Science* **2008**, 320, 1755-1759.

(9) Wendt, S.; Bechstein, R.; Porsgaard, S.; Lira, E.; Hansen, J. O.; Huo, P.; Li, Z.; Hammer, B.; Besenbacher, F. Comment on **"**Oxygen Vacancy Origin of the Surface Band-Gap State of TiO_2(110)**"**. *Phys. Rev. Lett.* **2010**, 104 (25), 259703**–**259703.

(10) Yim, C. M.; Pang, C. L. and Thornton, G. Oxygen Vacancy Origin of the Surface Band-Gap State of TiO_2(110). *Phys. Rev. Lett.* **2010**, 104 (3), 036806-1-4.

(11) Mao, X.; Lang, Z.; Wang, Z.; Hao, Q.; Wen, B.; Ren, Z.; Dai, D.; Zhou, C.; Liu, L-M. and Yang, X. Band-Gap States of TiO_2(110): Major Contribution from Surface Defects. *J. Phys. Chem. Lett.* **2013**, 4, 3839-3844.

(12) Tomkiewicz, M. The Potential Distribution at the TiO_2 Aqueous Electrolyte Interface. *J. Electrochem. Soc.* **1979**, 126 (9), 1505-1510.

(13) Siripala, W. and Tomkiewicz, M. Direct Observation of Surface States at the TiO2 Electrolyte Interface. *J. Electrochem. Soc.* **1981**, 128 (11), 24912492.

(14) Kobayashi, K.; Aikawa, Y. and Sukigara, M. Surafce State at semiconductorliquid junction. *J. Appl. Phys.* **1983**, 54 (5), 2526-2532.

(15) Kobayashi, K.; Ikeuchi, M. and Okada, G. Appearance of surface states at the TiO_2/H_2O interface after deposition of Fe atoms on the TiO_2 surface. *Chem. Phys. Lett.* **1990**, 174 (2), 157-161.

(16) Matsumoto, Y.; Takata, S.; Tanaka, R. and Hachiya, A. Electrochemical impedance analysis of electric field dependence of the permittivity of $SrTiO_3$ and TiO_2(110) single crystals. *J. Appl. Phys.* **2011**, 109, 014112-1-4.

(17) Stickney, J. L.; Rosasco, S. D.; Song, D.; Soriaga, M. P. and Hubbard, A. T. Superlattices formed by electrodeposition of silver on iodine-pretreated Pt(111); studies by LEED, Auger spectroscopy and electrochemistry. Surf. Sci. **1983**, 130 (2), 326-347.

(18) Taniguchi, M.; Kuzembaev, E.; Tanaka, K. A mimic model of Pt-Rh catalyst prepared by electrochemical deposition of Rh on the Pt(110) surface. *Surf. Sci.* **1993,** 290 (3), L711-L717.

(19) Yamada, T.; Batina, N. and Itaya, K. Interfacial structure of iodine electrodeposited on Au(111): studied by LEED and in situ STM. *Surf. Sci.* **1995**, 335, 204-209.

(20) Reniers, F. J. The development of a transfer mechanism between UHV and electrochemistry environments. *Phys. D: Appl. Phys*. **35**, R169 (2002).

(21) Takata, S.; Tanaka, R.; Hachiya, A. and Matsumoto, Y. Nanoscale Oxygen Nonstoichiometry in Epitaxial TiO_2 Films Grown by Pulsed Laser Deposition. *J. Appl. Phys.* 2011, 110, 103513-1-5.

(22) Miura, Y.; Takata, S. and Matsumoto, Y. Nondestructive and repeatable capacitance-voltage and current-voltage measurements across the oxide/electrolyte interface by UHV-electrochemistry approach. Appl. Phys. Exp. 2014, 7, 095802-1-4.

(23) Yamamoto, Y.; Nakajima, K.; Ohsawa, T.; Matsumoto, Y. and Koinuma, H. Preparation of Atomicalyy Smooth TiO_2 Single Crystal Surfaces and Their Photochemical Propweties. *Jpn. J. Appl. Phys*. **2005,** 44, L511-L514.

(24) Takata, S.; Hachiya, A. and Matsumoto, Y. Non-linear electric field response of permittivity of atomically smooth TiO2(rutile) single crystals studied by an electrochemical approach. *J. of Ceram. Soc. of Jpn.* **2012**, 120 (9), 366-369.

(25) Sawaguchi, E.; Kikuchi, A. and Kodera, Y. Dielectric Constant of Strontium Titanate at Low Temperatures. *J. Phys. Soc. Jpn*. **1962**, 17(10), 1666-1667.

(26) Oliva, F. Y.; Avalle, L. B.; Santos, E. and Camara, O. R. Photoelectrochemical characterization of nanocrystalline TiO2 films on titanium substrates. *J. Photochem. Photobiol. A* **2002**, 146, 175-188.

(27) Grant, F. A. Properties of Rutile (Titanium Dioxide). *Rev. Mod. Phys*. **1959**, 31 (3), 646-674.

(28) Reyren, N.; Thiel, S.; Caviglia, A. D.; Kourkoutis, L. F.; Hammeri, G.; Richter, C.; Schneider, C. W.; Kopp, T.; Rüestschi, A.-S.; Jaccard, D.; Gabay, M.; Muller, D. A.; Triscone, J.-M. and Mannhart, J. Superconducting Interfaces Between Insulating Oxides. Science 2007, 317 (5842), 1196-1199.

(29) Yamada, Y.; Ueno, K.; Fukumura, T.; Yuan, H. T.; Shimotani, H.; Iwasa, Y.; Gu, L.; Tsukimoto, S.; Ikuhara, Y. and Kawasaki, M. Electrically Induced Ferromagnetism at Room Temperature in Cobalt-Doped Titanium Dioxide. *Science* **2011**, 332 (6033), 1065-1067.

(30) Ohotomo, A. and Hwang, H. Y. A high-mobility electron gas at the $LaAlO_3/SrTiO_3$ heterointerface. *Nature* **2003**, 427, 423-426.

Figures & Captions

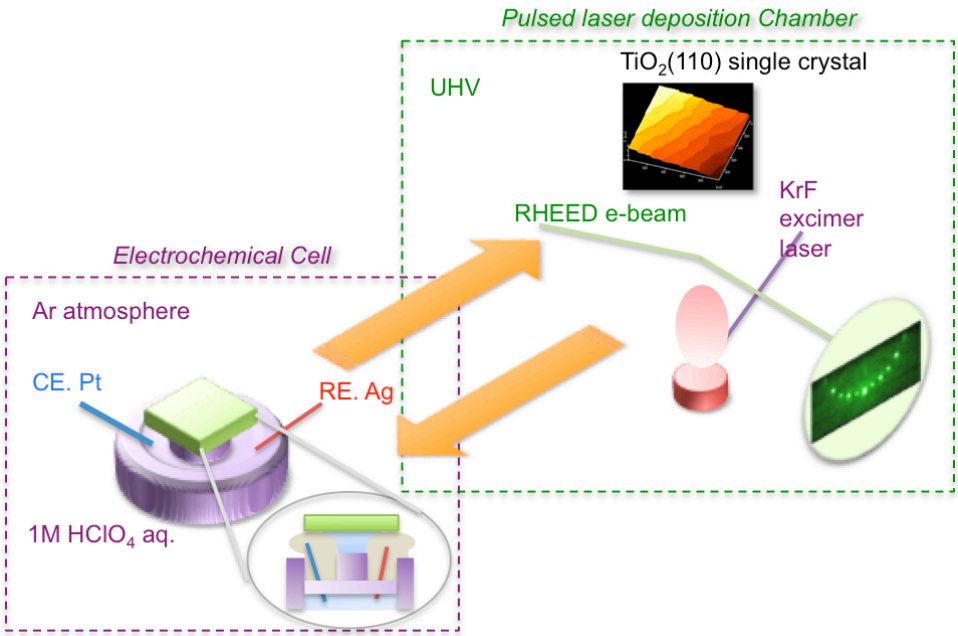

Figure 1. A schematic of in situ pulsed laser deposition-electrochemical cell (PLD-EC) system that has been originally developed in our group. A 0.5wt% Nb-doped TiO_2(110) single crystal sample that exhibits a steps-and-terraces structure as shown in AFM image, is used and it can be transferred back and forth between the PLD and EC chambers without exposure to air. In the PLD chamber, not only the TiO_2 sample surface preparation by annealing at various O_2 pressure conditions, but also the growth of epitaxial TiO_2 films can be made, together with a RHEED intensity monitoring system for controlling the layer-by-layer growth of films as well as for observing the surface cleanness and crystallinity of single crystal and growing oxide films. In the EC chamber, all the electrochemical measurements were performed in pure Ar gas at normal pressure, using a threeelectrode electrochemical cell with Ag and Pt wires as reference and counter electrodes, and an electrolyte solution of 1 M $HClO_4$. Mott-Schottky plots were measured at different modulation frequencies and an amplitude of 10 mV with an Ivium CompactStat electrochemical and impedance analyzer.

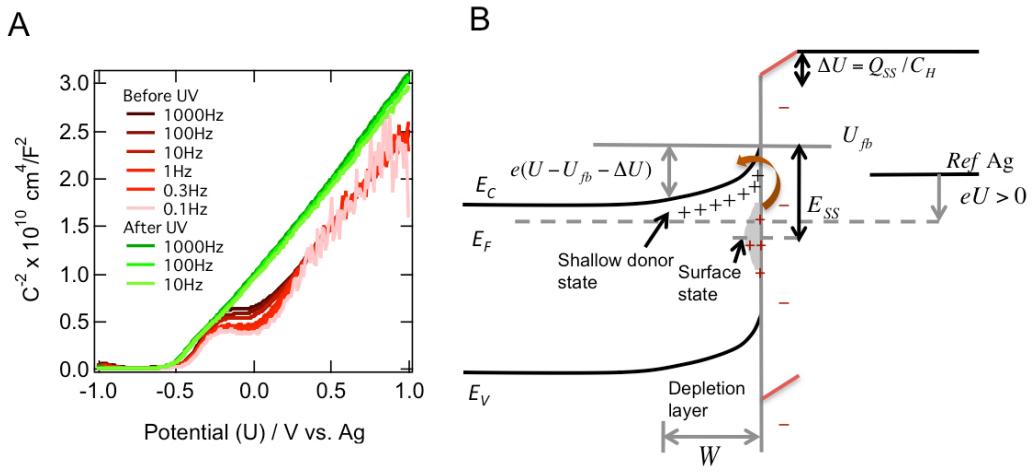

Figure 2. A set of Mott-Schottky plots of this TiO_2(110)-(1×1) surface was obtained for various modulation frequencies before and after UV illumination based on the equivalent series *RC* circuit (A), together with a schematic of the band diagram to illustrate the surface state in the band gap at the TiO_2/electrolyte interface (B). The nonlinear Mott-Schottky plots were observed in an electrode potential range of -0.25 to +0.25 V vs. Ag for the as-prepared clean TiO_2(110)-(1×1). This is attributed to a deep surface state in the band gap, whose frequency dependence indicates that the trap-detrap response of the deep surface state seems not to be able to follow at higher frequencies above 1000Hz. After UV illumination, such a nonlinear part in the Mott-Schottky plots completely disappeared, showing almost no frequency dependence as far as measured in the preset frequency range, which is due to the photoetching.

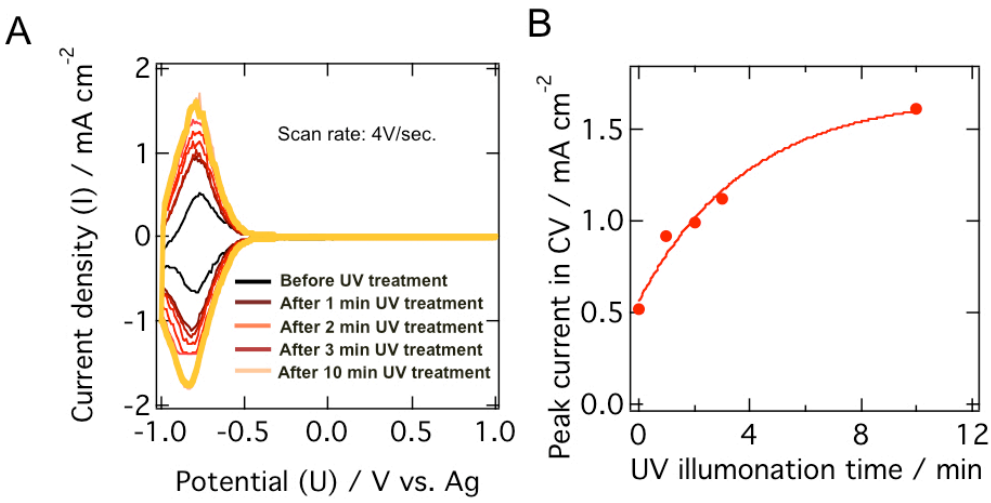

Figure 3. A set of the cyclic voltammograms (CVs) recorded at a scan rate of 4V/sec for each step of UV illumination. As the illumination time increased, the values of current density for the CV pair peaks at electrode potentials of about -0.8V vs. Ag, which may be assigned to the redox reaction of Ti(III) (hydr)oxide / Ti(IV) (hydr)oxide, was found to gradually increase. The current increase is attributed to the increase of the effective area of the electrode surface due to the surface roughening during the photoetching.

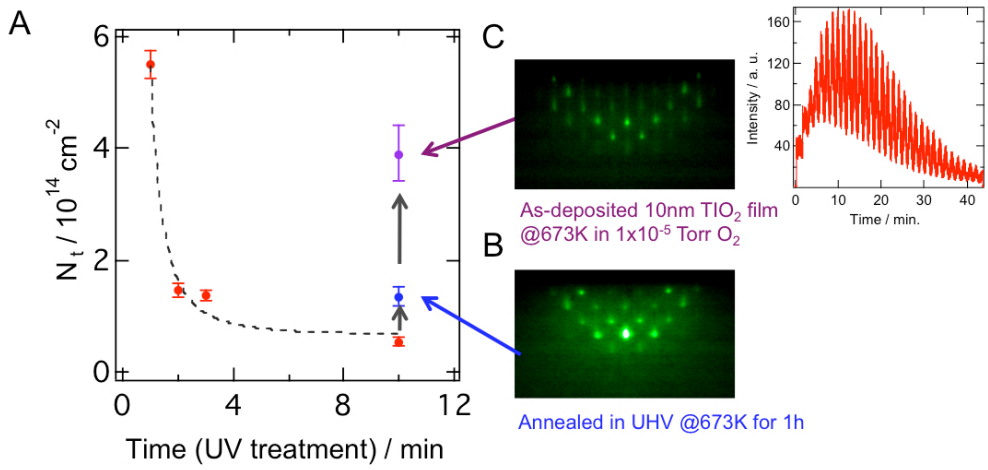

Figure 4. A series of the defect density changes during the step-by-step photoetching process of Fig. 3 (A) and the subsequent reduction (B) and growing film (C) treatments. The defect density systematically decreased during the photoetching by almost one order of magnitude. The photetched sample was then reduced by annealing at 673K in UHV, resulting in a slight increase of the defect density, and a much further increase by the subsequent growth of 10nm-thick TiO_2 at 673K in 1×10^{-5} Torr O_2, where the deposition condition was optimized so that the layer-by-layer growth was attained as observed by RHEED intensity oscillation (in the inset).

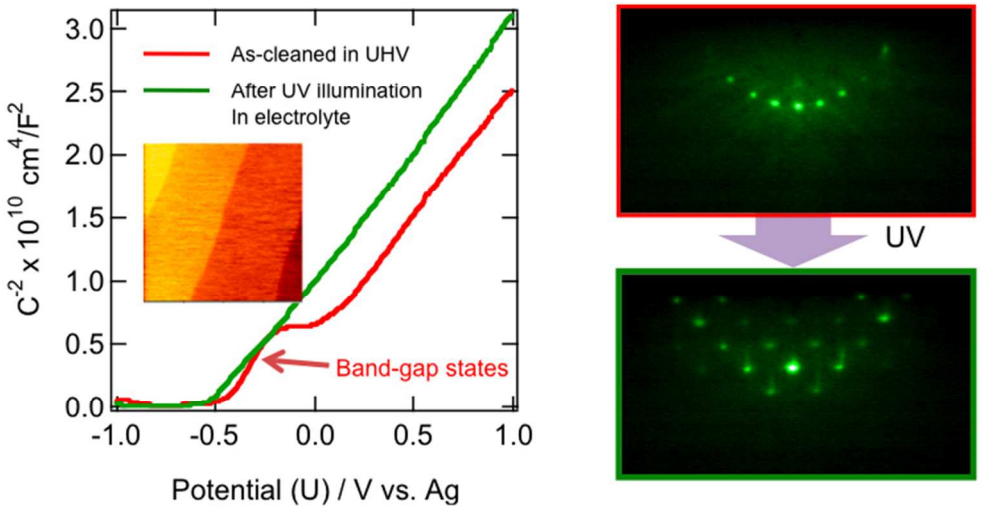

The intrinsic nature of band-gap states of UHV-clean TiO2(110) single crystal and film surfaces were electrochemically investigated by UHV-electrochemistry approach.
128x67mm (150 x 150 DPI)